

## FDA approved calcium channel blockers inhibit SARS-CoV-2 infectivity in epithelial lung cells

Marco R. Straus<sup>1</sup>, Miya Bidon<sup>2</sup>, Tiffany Tang<sup>2</sup>, Gary R. Whittaker<sup>1\*</sup> and Susan Daniel<sup>2\*</sup>

<sup>1</sup>Department of Microbiology and Immunology, Cornell University, Ithaca, NY, 14853, USA

<sup>2</sup>Robert Frederick Smith School of Chemical and Biomolecular Engineering, Cornell University, Ithaca, NY, 14853, USA

\*Corresponding authors:

Gary Whittaker: [grw7@cornell.edu](mailto:grw7@cornell.edu)

Susan Daniel: [sd386@cornell.edu](mailto:sd386@cornell.edu)

### Abstract

COVID-19 has infected more than 22 million people worldwide causing over 750,000 deaths. The disease is caused by the severe acute respiratory syndrome coronavirus (CoV) 2 (SARS-CoV-2), which shares a high sequence similarity to SARS-CoV. Currently there are no vaccinations available to provide protection and the only antiviral therapy in active use in patients is remdesivir, which currently provides only limited benefit. Hence, there is an urgent need for antiviral therapies against SARS-CoV2. SARS-CoV requires Ca<sup>2+</sup> ions for host cell entry and based on the similarity between SARS-CoV and SARS-CoV-2 it is highly likely that the same requirements exist for the two viruses. Here, we tested whether FDA-approved calcium channel blocker (CCB) drugs are efficacious to inhibit the spread of SARS-CoV-2 in cell culture. Our data shows that amlodipine, felodipine, and nifedipine limit the growth of SARS-CoV-2 in epithelial kidney (Vero E6) and epithelial lung (Calu-3) cells. We observed some differences in the inhibition efficacy of the drugs in the two different cell lines, but with felodipine and nifedipine having

the greatest effect. Overall, our data suggest that CCBs have a high potential to treat SARS-CoV-2 infections and their current FDA approval would allow for a fast repurposing of these drugs.

## **Introduction**

Coronaviruses (CoVs) are major zoonotic pathogens that cause respiratory and/or enteric tract infections in a variety of species, including humans. Most CoVs that are pathogenic to humans cause only mild cold-like disease symptoms[1]. However, currently the worldwide COVID-19 pandemic is caused by the severe acute respiratory syndrome (SARS) CoV 2 and poses a dramatic risk to public health worldwide[2]. The virus was first identified in December 2019 in Wuhan, China and since has spread all over the globe[3]. To date, there are no vaccines or highly efficacious drugs available against SARS-CoV-2.

Remdesivir, initially developed for Ebola treatment, is currently the only antiviral therapy used to effectively treat COVID-19 patients and was shown to improve symptoms in 68% of treated patients in clinical trials[4,5]. However, with only one efficacious antiviral therapy on the market, there remains a need to identify and to provide additional drugs that can treat COVID-19 patients. Given the current pandemic and the need for expediency, these drugs should ideally be FDA approved so they can be rapidly repurposed for COVID-19 treatment.

A promising target for a potential drug is a crucial step in the viral life cycle, such as the entry of the virus into the host cells[6]. Previous studies have revealed that SARS-CoV and MERS-CoV utilize calcium ions ( $\text{Ca}^{2+}$ ) for viral entry that are coordinated by amino acid residues within the fusion peptide of their Spike (S) proteins[7,8]. Depleting intracellular and/or extracellular  $\text{Ca}^{2+}$  resulted in full suppression of viral entry for SARS-CoV and partial reduction of viral fusion of MERS-CoV. Sequence comparisons show

that the fusion domains of SARS-CoV and SARS-CoV-2 are virtually identical, strongly suggesting that the same  $\text{Ca}^{2+}$ -dependency for viral entry exists for SARS-CoV-2[6].

The crucial role of  $\text{Ca}^{2+}$  in the viral entry of CoVs prompted us to explore whether FDA approved  $\text{Ca}^{2+}$  channel blocker (CCB) drugs have the potential to inhibit viral growth of SARS-CoV-2. We chose five drugs from different classes that all inhibit high voltage-activated  $\text{Ca}^{2+}$  channels of the L-type. We selected the dihydropyridines: amlodipine, nifedipine and felodipine; the phenylalkylamine: verapamil; and the benzothiazepine: diltiazem. These five drugs are primarily used to treat cardio-vascular diseases. In addition, we also tested the FDA-approved  $\text{Ca}^{2+}$  chelator drug: diethylenetriaminepentaacetic acid (DTPA), which is used to treat radioactive contamination of internal organs.

## Results

### **Amlodipine, nifedipine, felodipine and verapamil inhibit SARS-CoV-2 infection of Vero E6 cells**

We infected Vero E6 cells at a MOI of 0.1 and added four different concentrations of each compound immediately post infection (10  $\mu\text{M}$ , 50  $\mu\text{M}$ , 100  $\mu\text{M}$  and 500  $\mu\text{M}$ ). Viral titers were analyzed 24 hours post infection. For amlodipine, we observed a 5-log reduction of viral growth at 50  $\mu\text{M}$  and we were not able to detect any viral titer at a concentration of 100  $\mu\text{M}$  (Figure 1A). However, amlodipine also exhibited a 25% reduction of cell viability at a concentration of 50  $\mu\text{M}$ , which increased to 90% at 100  $\mu\text{M}$  and 500  $\mu\text{M}$  (Figure 2A). Nifedipine reduced viral titers by 5 logs at 500  $\mu\text{M}$  and expressed about 15% cytotoxicity (Figure 1A and 2A). Felodipine completely suppressed growth of SARS-CoV-2 at a concentration of 50  $\mu\text{M}$  with no statistically significant cytotoxicity. 100  $\mu\text{M}$  verapamil reduced the viral titers by 50% compared to the untreated control without a cytotoxic effect. Diltiazem reduced viral growth at 500  $\mu\text{M}$  but also compromised cell viability at this concentration and DTPA showed no effect.

### **Nifedipine and felodipine suppress SARS-CoV-2 infection of epithelial lung cells**

Vero E6 cells are a good model system for SARS-CoV-2 infections, but the cell line is derived from epithelial kidney cells and may not represent the virus-drug-cell interactions in the lung. Therefore, we tested the CCBs and DTPA in the epithelial lung cell line Calu-3 (Figure 1B). The results for amlodipine were comparable to what we found in Vero E6 cells (Figure 1 and 2). Nifedipine and felodipine, however, significantly inhibited viral growth at lower concentrations compared to Vero E6 cells. Nifedipine reduced the viral titers by 1.5 logs at a concentration of 100  $\mu$ M and no virus was detectable at 500  $\mu$ M while cytotoxicity was moderate. Felodipine diminished SARS-CoV-2 growth by half at 10  $\mu$ M and at 50  $\mu$ M no virus was detected with no cytotoxic effect on the cells. In contrast, verapamil had a weakened inhibitory effect at 100  $\mu$ M compared to Vero E6 cells. As in Vero E6 cells, 100  $\mu$ M verapamil fully suppressed viral growth but also compromised cell viability by about 90%. We found very modest infection inhibition for diltiazem and DTPA at non-cytotoxic concentrations of 500  $\mu$ M and 100  $\mu$ M, respectively (Figure 1B and 2B).

While these results are promising, it is unclear how the efficacious doses of amlodipine, nifedipine and felodipine found here would translate into clinical use in human patients to treat COVID-19 infections. But a recent report suggests that amlodipine and nifedipine reduce mortality and the risk for intubation in COVID-19 patients[9] and hence, provides an encouraging example that CCBs could be a viable option to fight COVID-19 infections.

It is important to emphasize that felodipine and nifedipine work with higher efficiency in Calu-3 cells compared to Vero E6 cells (Figure 1). In this context, it is noteworthy that CCBs are believed to affect airway smooth muscle cells, which rely on L-type calcium channels for their contraction[10–12]. Recently, the same CCBs tested here were shown to have a beneficial effect on the lung function of asthma patients, providing evidence that CCBs act in the lungs[13]. More evidence that interference with the cellular  $\text{Ca}^{2+}$  balance suppresses viral growth comes from nebulizers used for asthma medications. Nebulizers are supplemented with EDTA as a preservative, which may help to deplete

extracellular  $\text{Ca}^{2+}$  <sup>27</sup> and provide a clue as to why asthma is not on the top ten list of chronic health problems of people who died of COVID-19.

### **Inhibition may occur at the level of host cell entry**

The observed inhibition differences in these two cell lines suggest that inhibition may occur at the level of host cell entry. In Vero cells, CoVs preferentially enter the host cells via the endocytic pathway [6,14]. Calu-3 cells, on the contrary, are predominantly infected via plasma membrane fusion[6,15]. To further investigate whether CCB-mediated inhibition of SARS-CoV-2 infectivity affects viral host cell entry, we utilized murine leukemia virus (MLV)-based pseudo particles (PP) that were decorated with the SARS-CoV-2 S protein[16]. These virion surrogates allow for only one infection cycle without intracellular replication and thus, inhibition of PP infection would suggest that the CCBs affect host cell entry.

We pretreated all cells with the CCBs and DTPA for one hour before adding PPs carrying the SARS-CoV-2 S protein (Figure 3). Amlodipine suppressed PP infection at 50  $\mu\text{M}$  in both, Vero E6 and Calu-3 cells (Figure 3). Nifedipine inhibited PP infection in Vero E6 and Calu-3 cells with 500  $\mu\text{M}$  having the strongest effect. Felodipine inhibited PP entry in both cell lines at 50  $\mu\text{M}$ . Consistent with what we found in the live virus infection study above, verapamil suppressed PP entry at 50  $\mu\text{M}$  in Calu-3 and at 100  $\mu\text{M}$  in Vero E6 cells. In contrast to our observations with SARS-CoV-2 live virus infections, diltiazem and DTPA also inhibited PP infections (Figure 1 and 3). Diltiazem inhibited PP infection in Calu-3 starting at 50  $\mu\text{M}$ , and in Vero E6, at 500  $\mu\text{M}$ . DTPA had a much stronger effect, suggesting that it might be able to chelate  $\text{Ca}^{2+}$  ions in the extracellular space, and thus, prevent fusion of S with the membrane as previously described for SARS-CoV PPs in the presence of EGTA[7]. The applied DTPA concentrations, however, seem sufficient to prevent a single host cell entry, but incapable of inhibiting SARS-CoV-2 spread over several rounds of viral replication under the conditions used here.

### **CCBs have a high potential to treat COVID-19 patients**

There is evidence from previous reports that CCBs inhibit viral infections at the cell entry level. Influenza A infections, for example, trigger an influx of  $\text{Ca}^{2+}$  which assists the endocytic uptake of the virus, while treatment with verapamil or diltiazem inhibits viral infection[17–19]. New World hemorrhagic fever arenaviruses, such as the Junin virus, are reportedly sensitive to CCBs and treatment with CCBs blocks the entry of the virus into the host cell[20]. However, the exact mechanism of how CCBs suppress SARS-CoV-2 infection needs to be addressed in a follow up study. CCBs were also shown to interfere with viral replication of several other viruses (*e.g.*, Japanese Encephalitis virus, Zika virus, Dengue virus)[21]. Hence, while our results point to an interference of SARS-CoV-2 at host cell entry, it is conceivable that CCB-mediated inhibition of viral spread occurs at other stages as well, including viral release. Regardless of the exact mechanism, these examples demonstrate that CCBs exhibit an antiviral efficacy against a broad range of viral pathogens relevant for public health. They also show the broad requirement of  $\text{Ca}^{2+}$  ions for viral propagation, supported by other studies that report a  $\text{Ca}^{2+}$  requirement for major human pathogens like Ebola virus and Rubella virus[22,23]. Therefore, CCBs represent a novel class of antiviral therapeutics against a broad range of major viral diseases that warrant further clinical studies, but especially to address the current crisis of Covid-19.

## Figure legends

**Figure 1: Inhibitory effect of five CCBs and the  $\text{Ca}^{2+}$  chelator DTPA on SARS-CoV-2 infection.** (A) Vero E6 epithelial kidney cells were infected with SARS-CoV-2 isolate USA-WA1/2020 at a MOI of 0.1 for 24 hours. (B) Calu-3 epithelial lung cells were infected with SARS-CoV-2 isolate USA-WA1/2020 at a MOI of 0.1 for 24 hours. The CCBs amlodipine, nifedipine, felodipine, verapamil and diltiazem and the chelator DTPA were added to the cells at the indicated concentrations immediately after the virus. TCID50s were performed with growth supernatants and calculated according to the Reed-Muench method[24]. No bar

means no virus was detected at the respective concentration. Error bars represent standard deviations (n = 3). Asterisks indicate statistical significance compared to the untreated control. Statistical analysis was performed using an unpaired Student's t-test. \* = P > 0.05, \*\* = P > 0.01, \*\*\* = P > 0.001.

**Figure 2: Cytotoxic effect of the five CCBs and the Ca<sup>2+</sup> chelator DTPA on cells.** (A) Vero E6 epithelial kidney cells and (B) Calu-3 epithelial lung cells were treated with the indicated concentrations of amlodipine, nifedipine, felodipine, verapamil, diltiazem and DTPA for 24 hours. After 24 hours cell viability was measured using 3-(4,5-dimethylthiazol-2-yl)-2,5-diphenyltetrazolium bromide (MTT). Cell viability was determined by normalizing absorbance from the sample well by the average absorbance of untreated wells. Error bars represent standard deviations (n = 3). Asterisks indicate statistical significance compared to the untreated control. Statistical analysis was performed using an unpaired Student's t-test. \* = P > 0.05, \*\* = P > 0.01, \*\*\* = P > 0.001.

**Figure 3: Pseudo particle assays of SARS-CoV-2 S in Vero E6 and Calu-3 cells.** (A) Vero E6 epithelial kidney cells and (B) Calu-3 epithelial lung cells were pre-treated with CCBs and DTPA for one hour prior to infection with PPs carrying SARS-CoV-2 S. After 24 hours growth medium was changed and replenished with the drugs. 72 hours after infection the luciferase activity was assessed. Infectivity was normalized to the untreated sample. Error bars represent standard deviations (n = 3). Asterisks indicate statistical significance compared to the untreated control. Statistical analysis was performed using an unpaired Student's t-test. \* = P > 0.05, \*\* = P > 0.01, \*\*\* = P > 0.001.

## Methods

### Cells and reagents

Vero E6 and Calu-3 cells were obtained from the American Type Culture Collection (ATCC). Cells were maintained in Dulbecco's modified Eagle medium (DMEM) (Cellgro) supplemented with 25 mM HEPES (Cellgro) and 10% HyClone FetalClone II (GE) at 37° C and 5% CO<sub>2</sub>. For virus infections, cells were grown in Eagle's Minimum Essential Medium (EMEM) (Cellgro) supplemented with 4% heat inactivated fetal bovine serum (FBS) (Gibco) at 37° C and 5% CO<sub>2</sub>.

The SARS-CoV-2 isolate USA-WA1/2020 was obtained from the Biological and Emerging Infections Resources Program (BEI Resources). Amlodipine, nifedipine, felodipine, verapamil, diltiazem and DTPA were purchased from Sigma Aldrich. 3-(4,5-dimethylthiazol-2-yl)-2,5-diphenyltetrazolium bromide (MMT) was obtained from Thermo Fisher. Crystal violet was purchased from VWR. pCDNA3.1/SARS-CoV-2 S Wuhan Hu-1 was generously provided by Dr. David Veessler.

#### **SARS-CoV-2 infections and TCID50 assays**

Vero E6 and Calu-3 cells were grown to confluency under biosafety level-2 (BSL-2) conditions. Cells were then transferred to the BSL-3 lab, washed with DBPS and a volume of 200 µL infection media with SARS-CoV-2 at a MOI of 0.1 was added to the cells. Cells were then incubated at 37° C and 5% CO<sub>2</sub> for 1 hour on a rocker. Cells were then supplemented with 800 µL infection media and appropriate concentrations of each drug were added. Amlodipine, nifedipine, felodipine and verapamil were dissolved in DMSO. Therefore, DMSO was used as a control at the same volume that was applied for the highest drug concentration. After 24 hours, the supernatants were harvested and stored at -80° C.

For the TCID50, Vero E6 cells were grown to confluency in 96 well plates and serial dilution of the samples were prepared. Undiluted and diluted samples were then added to the Vero E6 cells and grown for 72 hours at 37° C and 5% CO<sub>2</sub>. After 72 hours supernatants were aspirated, and cells were fixed with 4% paraformaldehyde. Cells were then stained with 0.5% crystal violet and subsequently washed with



dH<sub>2</sub>O. Wells were scored and analyzed for living or dead cells according to the Reed-Muench method[24].

### **Cytotoxicity assay**

The cytotoxicity of the calcium ion blocking drugs (amlodipine, nifedipine, felodipine, diltiazem) and calcium chelator (DTPA) on VeroE6 and Calu-3 cells were determined by an MTT Assay. A total of  $5 \times 10^5$  VeroE6 cells/well, and  $6.7 \times 10^5$  Calu-3 cells/well were incubated in the presence of the six calcium blocking drugs and calcium chelator at the concentrations of 10, 50, 100, and 500  $\mu$ M for 24 hour at 37°C C and 5% CO<sub>2</sub> in a CO<sub>2</sub> incubator. After 24 hours incubation, cells were treated with MTT solution (5 mg/mL) and incubated for 4 hours at 37°C and 5% CO<sub>2</sub> with rocking to allow purple formazan crystals to form. 50  $\mu$ L DMSO was added into each well to dissolve the crystals. The absorbance was measured at 540 nm in a microplate reader (Bio-Tek Instrument Co., WA, USA).

### **Pseudo particle production and infections**

Pseudo particles production and infections were performed as previously described with minor modification[8]. For PP production, HEK 293T cells were transfected with pCDNA3.1/SARS-CoV-2 S Wuhan Hu-1 to generate SARS-CoV-2 S carrying PPs. Supernatants were harvested 72 hours post transfection and stored at -80°C. For infections, cells were seeded in 96-well plates and DMEM containing the different CCBs and DTPA was added and incubated for 1 hour. After one hour 50  $\mu$ L PPs were added. After 24 hours, cells were replenished with DMEM containing the individual drugs at the appropriate concentration and incubated for another 48 hours. After lysis, luciferase activity was measured using a GloMax Navigator Microplate Luminometer (Promega). Data was analyzed using Microsoft Excel and GraphPad Prism 8.

## References

1. Su S, Wong G, Shi W, Liu J, Lai ACK, Zhou J, et al. Epidemiology, Genetic Recombination, and Pathogenesis of Coronaviruses. *Trends in Microbiology*. Elsevier Ltd; 2016. pp. 490–502.  
doi:10.1016/j.tim.2016.03.003
2. World Health Organization. Coronavirus Disease 2019 (COVID-19) Situation Reports - 72. WHO Situat Rep. 2020. Available: <https://www.who.int/emergencies/diseases/novel-coronavirus-2019/situation-reports>
3. Wu F, Zhao S, Yu B, Chen YM, Wang W, Song ZG, et al. A new coronavirus associated with human respiratory disease in China. *Nature*. 2020;579: 265–269. doi:10.1038/s41586-020-2008-3
4. Grein J, Ohmagari N, Shin D, Diaz G, Asperges E, Castagna A, et al. Compassionate Use of Remdesivir for Patients with Severe Covid-19. *N Engl J Med*. 2020;382: 2327–2336.  
doi:10.1056/NEJMoa2007016
5. Boulware DR, Pullen MF, Bangdiwala AS, Pastick KA, Lofgren SM, Okafor EC, et al. A Randomized Trial of Hydroxychloroquine as Postexposure Prophylaxis for Covid-19. *N Engl J Med*. 2020 [cited 9 Jul 2020]. doi:10.1056/nejmoa2016638
6. Tang T, Bidon M, Jaimes JA, Whittaker GR, Daniel S, Frederick R. Coronavirus membrane fusion mechanism offers a potential target for antiviral development. 2020 [cited 9 Jul 2020].  
doi:10.1016/j.antiviral.2020.104792
7. Lai AL, Millet JK, Daniel S, Freed JH, Whittaker GR. The SARS-CoV Fusion Peptide Forms an Extended Bipartite Fusion Platform that Perturbs Membrane Order in a Calcium-Dependent Manner. *J Mol Biol*. 2017;429: 3875–3892. doi:10.1016/j.jmb.2017.10.017
8. Straus MR, Tang T, Lai AL, Flegel A, Bidon M, Freed JH, et al. Ca<sup>2+</sup> Ions Promote Fusion of Middle

- East Respiratory Syndrome Coronavirus with Host Cells and Increase Infectivity VIRUS-CELL INTERACTIONS crossm Downloaded from. *J Virol.* 2020;94: 426–446.  
doi:10.1128/JVI.00426-20
9. Solaimanzadeh I. Nifedipine and Amlodipine Are Associated With Improved Mortality and Decreased Risk for Intubation and Mechanical Ventilation in Elderly Patients Hospitalized for COVID-19. *Cureus.* 2020;12: e8069–e8069. doi:10.7759/cureus.8069
  10. Löfdahl C -G, Barnes PJ. Calcium, Calcium Channel Blockade and Airways Function. *Acta Pharmacol Toxicol (Copenh).* 1986;58: 91–111. doi:10.1111/j.1600-0773.1986.tb02525.x
  11. Du W, McMahon TJ, Zhang ZS, Stiber JA, Meissner G, Eu JP. Excitation-contraction coupling in airway smooth muscle. *J Biol Chem.* 2006;281: 30143–30151. doi:10.1074/jbc.M606541200
  12. Flores-Soto E, Reyes-García J, Sommer B, Montaña LM. Sarcoplasmic reticulum Ca<sup>2+</sup> refilling is determined by L-type Ca<sup>2+</sup> and store operated Ca<sup>2+</sup> channels in guinea pig airway smooth muscle. *Eur J Pharmacol.* 2013;721: 21–28. doi:10.1016/j.ejphar.2013.09.060
  13. Chiu KY, Li JG, Lin Y. Calcium channel blockers for lung function improvement in asthma: A systematic review and meta-analysis. *Ann Allergy, Asthma Immunol.* 2017;119: 518-523.e3. doi:10.1016/j.anai.2017.08.013
  14. Matsuyama S, Nagata N, Shirato K, Kawase M, Takeda M, Taguchi F. Efficient Activation of the Severe Acute Respiratory Syndrome Coronavirus Spike Protein by the Transmembrane Protease TMPRSS2. *J Virol.* 2010;84: 12658–12664. doi:10.1128/jvi.01542-10
  15. Kawase M, Shirato K, van der Hoek L, Taguchi F, Matsuyama S. Simultaneous Treatment of Human Bronchial Epithelial Cells with Serine and Cysteine Protease Inhibitors Prevents Severe Acute Respiratory Syndrome Coronavirus Entry. *J Virol.* 2012;86: 6537–6545.

doi:10.1128/jvi.00094-12

16. Millet JK, Tang T, Nathan L, Jaimes JA, Hsu HL, Daniel S, et al. Production of pseudotyped particles to study highly pathogenic coronaviruses in a biosafety level 2 setting. *J Vis Exp.* 2019;2019. doi:10.3791/59010
17. Fujioka Y, Tsuda M, Nanbo A, Hattori T, Sasaki J, Sasaki T, et al. A Ca<sup>2+</sup>-dependent signalling circuit regulates influenza A virus internalization and infection. *Nat Commun.* 2013;4: 1–13. doi:10.1038/ncomms3763
18. Nugent KM, Shanley JD. Verapamil inhibits influenza A virus replication. *Arch Virol.* 1984;81: 163–170. doi:10.1007/BF01309305
19. Fujioka Y, Nishide S, Ose T, Suzuki T, Kato I, Fukuhara H, et al. A Sialylated Voltage-Dependent Ca<sup>2+</sup> Channel Binds Hemagglutinin and Mediates Influenza A Virus Entry into Mammalian Cells. *Cell Host Microbe.* 2018;23: 809-818.e5. doi:10.1016/j.chom.2018.04.015
20. Lavanya M, Cuevas CD, Thomas M, Cherry S, Ross SR. siRNA screen for genes that affect Junín virus entry uncovers voltage-gated calcium channels as a therapeutic target. *Sci Transl Med.* 2013;5: 204ra131-204ra131. doi:10.1126/scitranslmed.3006827
21. Wang S, Liu Y, Guo J, Wang P, Zhang L, Xiao G, et al. Screening of FDA-Approved Drugs for Inhibitors of Japanese Encephalitis Virus Infection. *J Virol.* 2017;91. doi:10.1128/jvi.01055-17
22. Nathan L, Lai A, Millet J, Straus M, Whittaker GR, Freed JH, et al. Calcium ions directly interact with the Ebola virus fusion peptide to promote structure-function changes that enhance infection. *ACS Infect Dis.* 2019; acsinfecdis.9b00296. doi:10.1021/acsinfecdis.9b00296
23. Dubé M, Rey FA, Kielian M. Rubella Virus: First Calcium-Requiring Viral Fusion Protein. *PLoS Pathog.* 2014;10. doi:10.1371/journal.ppat.1004530

24. Lindenbach BD. Measuring HCV infectivity produced in cell culture and in vivo. *Methods Mol Biol.* 2009;510: 329–336. doi:10.1007/978-1-59745-394-3\_24

### **Acknowledgements**

This project was funded by Fast Grant, Mercatus Center. We would like to thank Paul Jeannette for his support for all the BSL-3 work and Dr. Bruce Kornreich and Dr. Hanno Andreas Ludewig for their critical input. TT is supported by the National Science Foundation Graduate Research Fellowship Program under Grant No. DGE-1650441.

### **Author contributions**

MRS: study design, experimental execution, data analysis, writing and editing of the manuscript. MB: experimental execution and data analysis. TT: experimental execution and data analysis. GRW: study design, writing and editing of the manuscript. SD: study design, writing and editing of the manuscript, funding acquisition.

Figures

Figure 1A

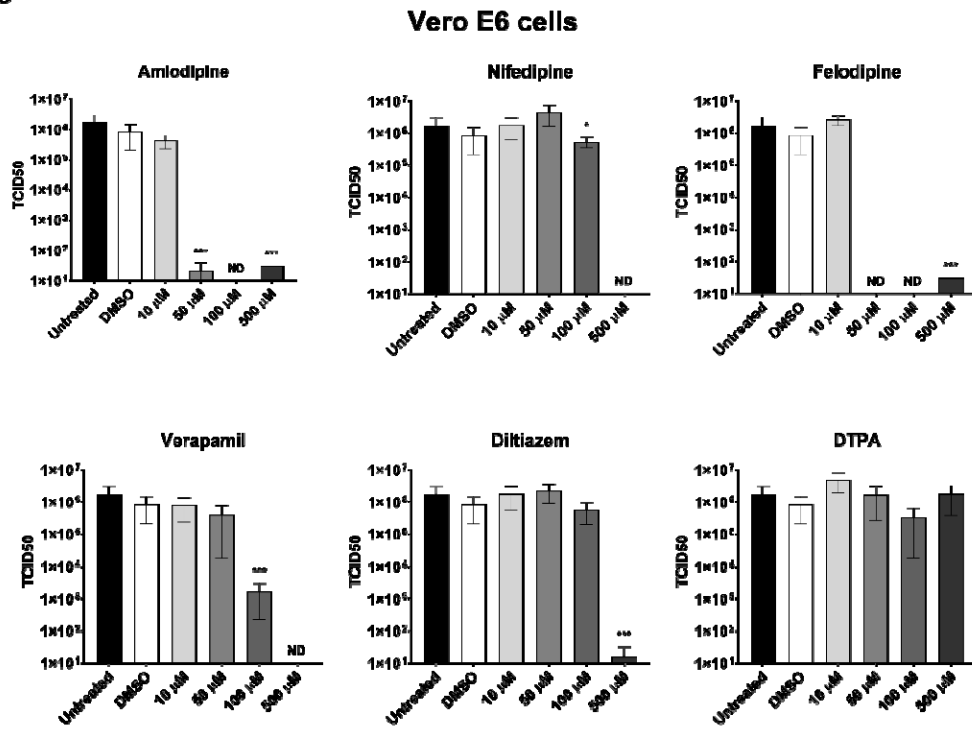
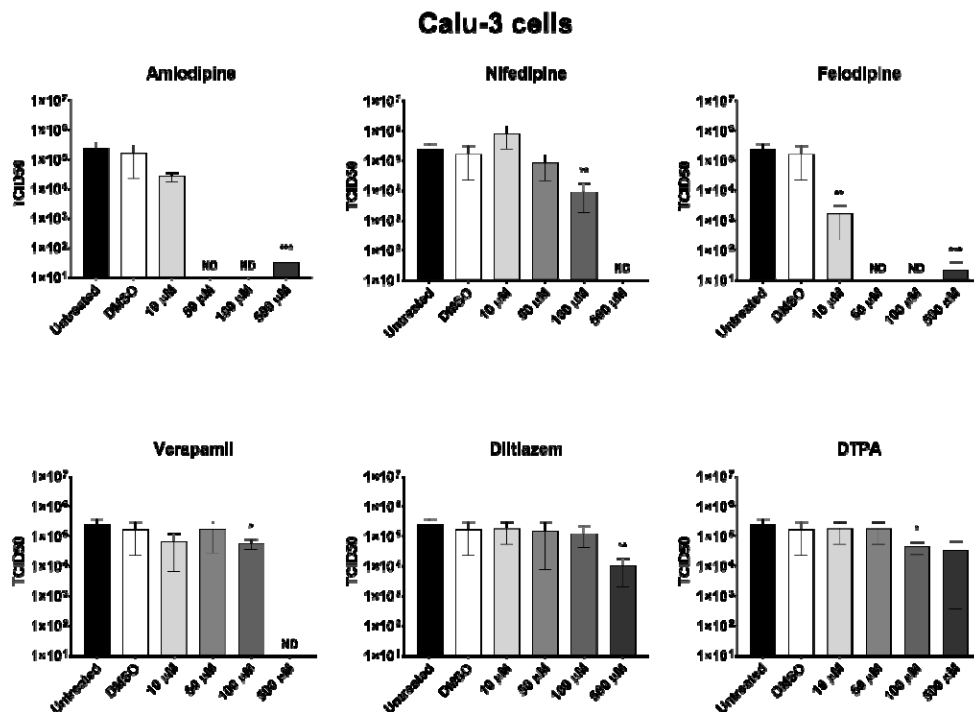
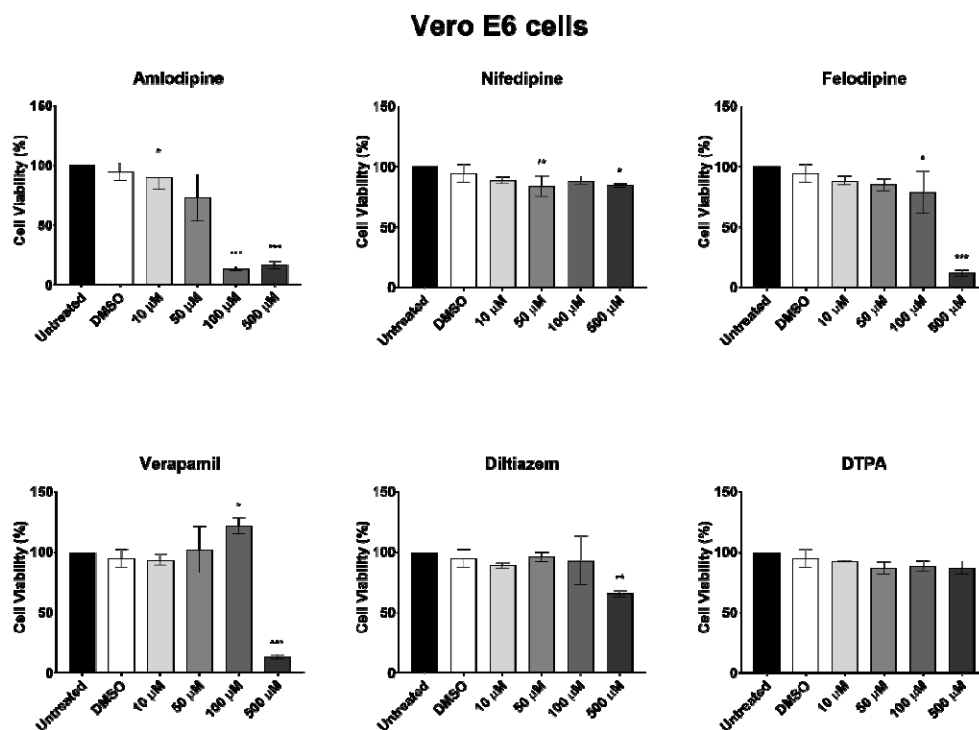


Figure 1B



**Figure 2A**



**Figure 2B**

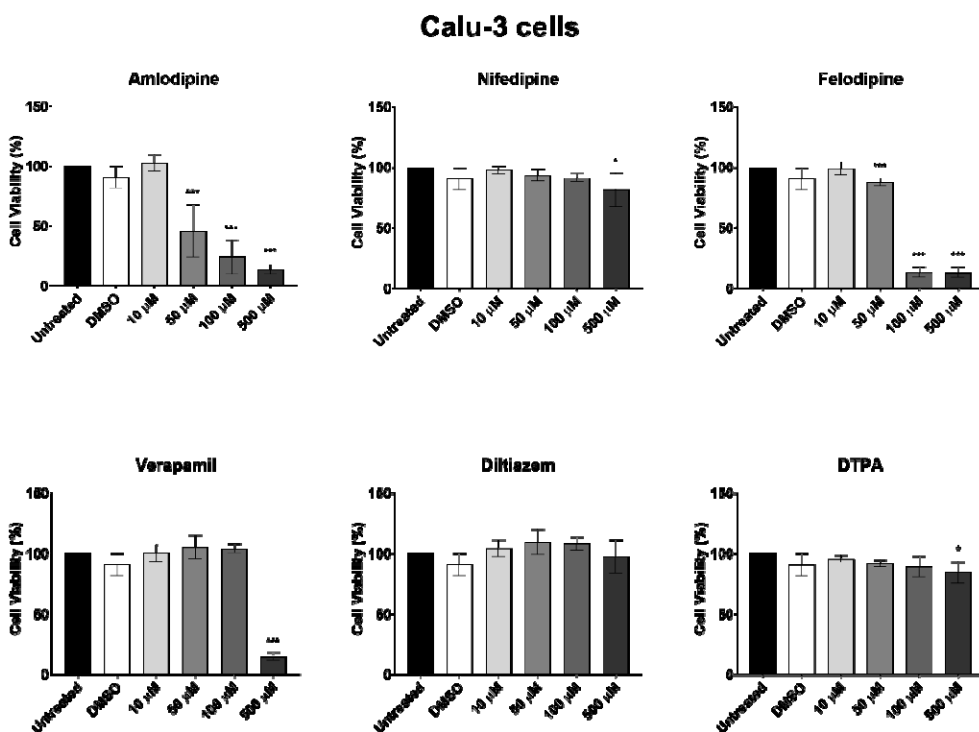


**Figure 3A**

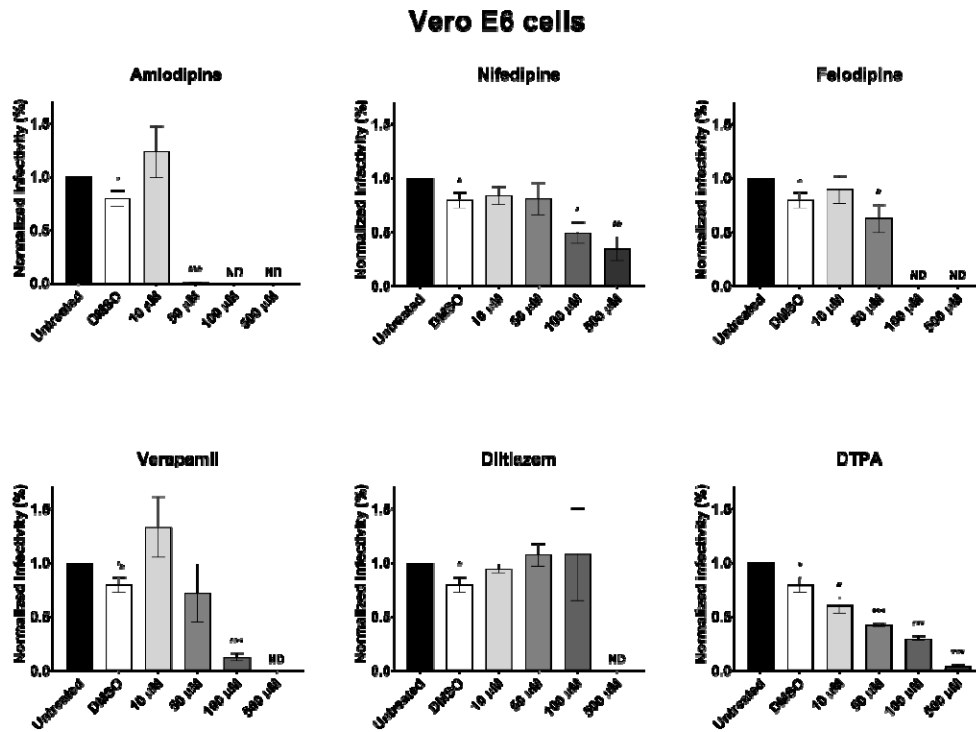


**Figure 3B**

